Tropospheric Formation of Hydroxymethyl Hydroperoxide, Formic Acid, H_2O_2, and OH from Carbonyl Oxide in the Presence of Water Vapor: A Theoretical Study of the Reaction Mechanism

Ramon Crehuet,[a] Josep M. Anglada,*[a] and Josep M. Bofill[b]

Abstract: We have carried out a theoretical investigation of the gas-phase reaction mechanism of the $H_2COO + H_2O$ reaction, which is interesting for atmospheric purposes. The B3LYP method with the 6-31G(d,p) and 6-311 + G(2d,2p) basis sets was employed for the geometry optimization of the stationary points. Additionally, single-point CCSD(T)/6-311 + G(2d,2p) energy calculations have been done for the B3LYP/6-311 + G(2d,2p) optimized structures. The reaction begins with the formation of a hydrogen-bond complex that we have calculated to be 6 kcal mol^{-1} more stable than the reactants. Then, the reaction follows two different channels. The first one leads to the formation of hydroxymethyl hydroperoxide (HMHP), for which we have calculated an activation barrier of $\Delta G_a(298) = 11.3$ kcal mol^{-1}, while the second one gives $HCO + OH + H_2O$, with a calculated activation barrier of $\Delta G_a(298) = 20.9$ kcal mol^{-1}. This process corresponds to the water-catalyzed decomposition of H_2COO, and its unimolecular decomposition has been previously reported in the literature. Additionally, we have also investigated the HMHP decomposition. We have found two reaction modes that yield $HCOOH + H_2O$; one reaction mode leads to $H_2CO + H_2O_2$ and a homolytic cleavage, which produces $H_2COOH +$ OH radicals. Furthermore, we have also investigated the water-assisted HMHP decomposition, which produces a catalytic effect of about 14 kcal mol^{-1} in the process that leads to $H_2CO + H_2O_2$.

Keywords: ab initio calculations · atmospheric chemistry · carbonyl oxide · reaction mechanisms · water chemistry

I. Introduction

Many degradation reactions of importance in tropospheric chemistry begin with the ozonolysis of alkenes. The reaction of ozone with terminal alkenes (such as isoprene, β-pinene, and other biogenic hydrocarbons) proceeds via the formation of a primary ozonide (1,2,3-trioxolane),(**1**) which decomposes to the Criegee intermediates (carbonyl oxide and aldehyde pair (**2**, **3**)) as two of the major products.

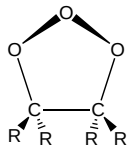

1 (POZ)

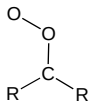

2

3

In the gas phase, carbonyl oxide (H_2COO) is formed with an excess of energy and may either, decompose unimolecularly (among 37–50%) or become collisionally stabilized (among 63–50%),[1–5] and then undergo bimolecular reactions with other tropospheric gases. The gas-phase unimolecular decomposition of H_2COO leads to the formation of HCOOH, CO_2, CO, H_2O, H_2, H, HCO, OH, H_2CO, and O.[4, 6–15] With respect to the stabilized carbonyl oxide, its reaction with water vapor is one of the most important reactions in atmospheric chemistry, and it is believed that it constitutes the major degradation reaction in the atmosphere.[16, 17] It is known that this reaction leads to the formation of hydroxymethyl hydroperoxide ($OHCH_2OOH$ or HMHP), formic acid, and H_2O_2.[18–23] These species are important in environmental chemistry. They have been

[a] Dr. J. M. Anglada, Dr. R. Crehuet
Institut d'Investigacions Químiques
i Ambientals de Barcelona
Departament de Química Orgànica Biològica
IIQAB-CSIC. C/Jordi Girona 18, 08034 Barcelona
Catalunya (Spain)
Fax: (+34) 932 045 904
E-mail: rcsqtc@iiqab.csic.es, anglada@iiqab.csic.es

[b] Dr. J. M. Bofill
Departament de Química Orgànica
and Centre de Recerca en Química Teòrica
Universitat de Barcelona, C/Martí i Franquès 1
08028 Barcelona, Catalunya (Spain)
E-mail: jmbofill@qo.ub.es

Supporting information for this article is available on the WWW under http://www.wiley-vch.de/home/chemistry/ or from the author.

  0947-6539/01/0710-2227 $ 17.50+.50/0

detected in air and precipitation and have been measured in rural, forested, and urban areas under polluted conditions.[24–30] It is also believed that these compounds have a direct impact on the control of plant growth and forest damage. HMHP may also act as an enzymatic inhibitor of peroxidases, while H_2O_2 is a very important oxidant.[31–33] Moreover, the reaction of carbonyl oxides with water is also important in drinking water and wastewater processes, in which ozonolysis is widely used.[34]

Several investigations have been carried out to explain the formation of HMHP, HCOOH, and H_2O_2 in the presence of water vapor.[18–23, 35–37] In a first stage, the reaction proceeds by the addition of the H_2O to the Criegee biradical, which leads to HMHP, and then it decays to give $HCOOH + H_2O$ or $H_2CO + H_2O_2$. However, in a recent study, Neeb et al.[21] found that the decomposition of HMHP results almost exclusively in $HCOOH + H_2O$, while the formation of $H_2CO + H_2O_2$ should be of minor importance.

Despite the importance of the reaction of carbonyl oxide with water, the detailed mechanism is not known. Therefore, in the present investigation we aim to shed light on it by means of a theoretical study. Thus, in a first step, we have considered the addition of one water molecule to formaldehyde carbonyl oxide, which leads to the formation of HMHP [Eq. (1)]. In a second step, we have studied the unimolecular decomposition of HMHP as shown in Equations (2)–(4). Furthermore, we have also considered the decomposition of HMHP assisted by a water molecule [Eqs. (5) and (6)] and finally, we have investigated an additional reaction mode between $H_2COO + H_2O$ that does not lead to the formation of HMHP but releases OH and HCO radicals [Eq. (7)].

$$H_2COO + H_2O \rightarrow H_2C(OH)OOH \quad (1)$$

$$H_2C(OH)OOH \rightarrow HCOOH + H_2O \quad (2)$$

$$H_2C(OH)OOH \rightarrow H_2O_2 + H_2CO \quad (3)$$

$$H_2C(OH)OOH \rightarrow H_2COOH + OH \quad (4)$$

$$H_2C(OH)OOH + H_2O \rightarrow HCOOH + 2H_2O \quad (5)$$

$$H_2C(OH)OOH + H_2O \rightarrow H_2O_2 + H_2CO + H_2O \quad (6)$$

$$H_2C(OH)OOH + H_2O \rightarrow HCO + OH + H_2O \quad (7)$$

II. Technical details: The geometry optimizations for all stationary points were performed by using the hybrid density functional B3LYP method.[38] In a first step, the geometries of each structure were fully optimized using the 6-31G(d,p) basis set.[39] The harmonic vibrational frequencies were also calculated to verify the nature of the corresponding stationary point (minima or transition states) and to provide the zero-point vibrational energy (ZPE) and the thermodynamic contributions to the enthalpy and free energy for $T = 298$ K. In order to take into account the anharmonicity effects, the ZPE energies were scaled by 0.9806.[40] Moreover, to ensure that the transition states connect the desired reactants and products, we have performed intrinsic reaction coordinate

Table 1. ZPE [kcal mol^{-1}], entropies S [e.u.], relative energies ΔE, relative enthalpies $\Delta H(298)$, relative free energies $\Delta G(298)$ [kcal mol^{-1}], and dipole moments [debye] for the optimized structures computed at B3LYP and CCSD(T) levels of theory using the 6-311 + G(2d,2p) basis set.[a]

Compound	Relative to	ZPE	S[b]	B3LYP ΔE	B3LYP ΔH	B3LYP ΔG	CCSD(T) ΔE	CCSD(T) ΔH	CCSD(T) ΔG	μ
$H_2COO + H_2O$		32.4	104.7	0.0	0.0	0.0	0.0	0.0	0.0	–
M1	**$H_2COO + H_2O$**	34.8	74.8	−8.2	−6.4	2.5	−8.8 −7.8[c]	−7.0 −6.0[c]	1.9 0.9[c]	3.1
TS1	**M1**	35.1	66.7	8.1	7.3	9.7	9.7	8.9	11.3	4.1
M2a	**TS1**	37.0	68.7	−43.5	−40.7	−41.3	−46.8	−44.1	−44.6	2.1
M2d	**M2a**	37.2	69.7	0.8	0.7	0.4	0.8	0.7	0.4	2.6
M2b	**M2a**	37.3	69.6	0.2	0.2	−0.1	0.2	0.2	−0.1	1.2
M2e	**M2a**	37.0	70.6	3.6	3.4	2.8	3.7	3.6	3.0	0.9
M2c	**M2a**	37.1	69.9	1.3	1.1	0.8	1.6	1.4	1.0	1.9
TS2	**M2d**	36.9	67.1	3.5	2.9	3.7	4.0	3.3	4.1	1.7
TS3	**M2b**	32.5	69.8	50.0	45.2	45.1	49.2	44.3	44.2	0.5
TS3a	**M2b**	32.2	70.2	53.3	48.3	48.0	52.6	47.5	47.4	3.0
TS4	**M2b**	32.3	66.5	47.9	42.4	43.3	52.7	47.2	48.2	1.5
TS5	**M2d**	32.8	70.0	48.1	43.7	43.6	52.0	47.5	47.5	3.1
$H_2COOH + OH$	**M2a**	30.8	106.4	40.4	35.1	23.8	44.4	39.0	27.8	–
$H_2O_2 + H_2CO$	**TS5**	32.7	106.7	−31.4	−30.2	−14.6	−34.5	−33.3	−44.2	–
***syn*-HCOOH + H_2O**	**TS3**	34.1	104.4	−121.5	−118.7	−129.0	−120.6	−117.7	−128.0	–
***anti*-HCOOH + H_2O**	**TS4**	33.8	104.6	−115.2	−112.0	−123.3	−119.9	−116.7	−128.0	–
TS6	**M2a + H_2O**	47.9	77.8	31.7	27.7	38.4	38.3	34.2	44.9	2.7
TS6a	**M2b + H_2O**	47.7	77.8	33.7	29.4	40.5	40.4	36.1	47.1	4.0
TS7	**M2c + H_2O**	47.1	75.7	31.0	26.1	37.8	38.6	33.6	45.3	3.2
TS7a	**M2d + H_2O**	47.4	76.1	42.2	37.5	49.1	40.2	35.5	47.1	1.2
TS8	**M2e + H_2O**	48.8	78.1	21.2	18.2	29.4	25.6	22.6	33.8	2.0
TS9	**M2a + H_2O**	48.9	73.4	31.2	27.6	39.6	33.1	29.5	41.5	2.0
TS10	**M1**	31.0	68.1	21.1	16.3	18.3	23.7	18.9	20.9	3.4
$HCO + OH + H_2O$	**TS10**	26.3	141.3	−18.2	−19.5	−41.3	−23.2	−24.5	−46.3	–

[a] The ZPE (scaled by 0.9806) and the thermodynamic contributions to enthalpy and free energy are computed at the B3LYP/6-31G(d,p) level of theory. The dipole moments are computed at the B3LYP/6-311 + G(2d,2p) level of theory. [b] The computed entropies S for the reactants and products are: 59.6 (H_2COO); 45.1 (H_2O); 63.8 (H_2COOH); 42.6 (OH); 54.5 (H_2O_2); 52.2 (H_2CO); 59.3 (*syn*-HCOOH); 59.5 (*anti*-HCOOH). [c] Includes the BSSE corrections.

0947-6539/01/0710-2228 $ 17.50+.50/0 *Chem. Eur. J.* **2001**, *7*, No. 10

calculations (IRC) at this level of calculation for each transition state. In a second step, all stationary points were reoptimized using the more flexible 6-311 + G(2d,2p) basis set.[41] Finally, we have performed single-point CCSD(T) calculations[42–44] using the 6-311 + G(2d,2p) basis set at the geometries obtained at B3LYP/6-311 + G(2d,2p) level of theory. Moreover, in order to obtain a better estimation of the stability of a complex structure found in this investigation, we have also computed the basis set superposition error (BSSE) according to the counterpoise method by Boys and Bernardi.[45] All calculations were done using the Gaussian 94 program package.[46]

Throughout the text, all geometry discussions will refer to the B3LYP/6-311 + G(2d,2p) values, and the energies will refer to those computed at CCSD(T)/6-311 + G(2d,2p)// B3LYP/6-311 + G(2d,2p). The ZPE and enthalpic corrections are calculated with the B3LYP/6-31G(d,p) values. Moreover, the relative energies computed at B3LYP/6-311 + G(2d,2p) are also tabulated for the sake of comparison. The Cartesian coordinates of all stationary points, their absolute energies, and the relative energies computed at B3LYP/6-31G(d,p) are also available as Supporting information.

III. Results and Discussion

In the text, the structures of the stationary points are designated by **M** for the minima and by **TS** for the transition states, followed by a number (**1**, **2** and so on). Moreover, in order to distinguish different conformational isomers, we have also added the letters **a**, **b**, and so on. The most relevant geometrical parameters of the calculated stationary points are shown in Figures 1–5 and 7–10, while the corresponding relative reaction and activation energies, enthalpies, and free energies are listed in Table 1. Throughout the text we will compare reaction channels that involve one water molecule with reaction channels that involve two water molecules, and consequently the entropic effects become important. Therefore, unless otherwise stated, free energies obtained with the larger basis set will be discussed throughout the paper. Figure 6 shows a schematic free-energy reaction diagram.

A) Formation of the hydrogen-bond complex: The reaction between H_2COO and H_2O begins with the formation of a hydrogen-bond complex that we have labeled as **M1** (Figure 1), and whose existence has been recently pointed out by Aplincourt et al.[47] Our calculations indicate that **M1** is 6 kcal mol^{-1} more stable than the reactants (including the BSSE corrections, see Table 1) and, taking into account the different entropic effects between **M1** and H_2COO plus H_2O ($\Delta S = -29.9$ e.u.), we have computed a $\Delta G_r^{\circ}(298)$ of 0.9 kcal mol^{-1}. After **M1** the reaction can follow two different channels, which involve the formation of HMHP via **TS1** and the production of OH and HCO radicals via **TS10**.

B) The formation of HMHP: After **M1**, the reaction goes on through **TS1** before the production of HMHP, and the corresponding minimum has been labeled as **M2a** (Figure 2). This path can be envisaged as a 1,3-dipolar interaction

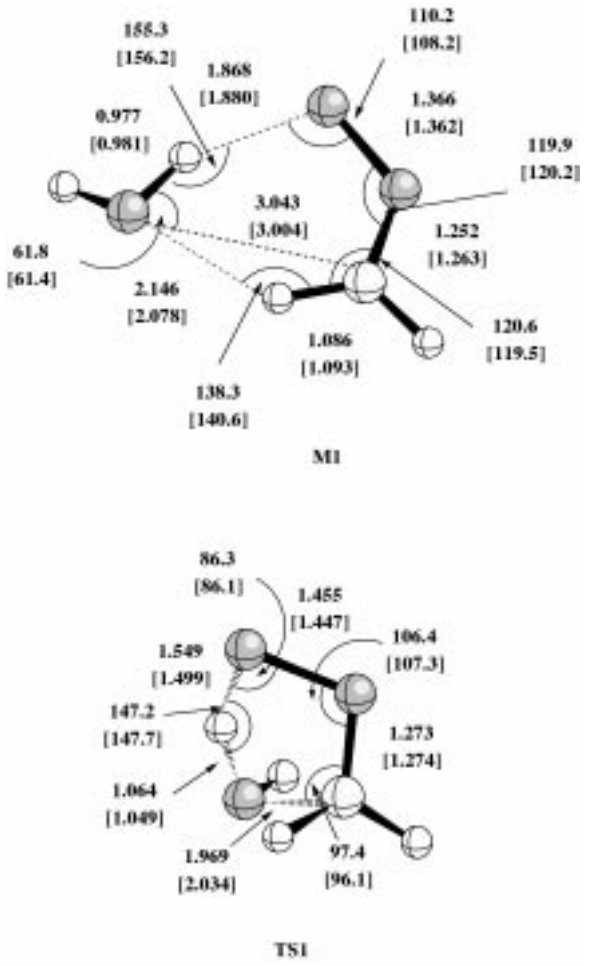

Figure 1. Selected geometrical parameters of the B3LYP/6-311 + G(2d,2p) and B3LYP/6-31G(d,p) (in brackets). **M1** and **TS1** for the stationary points of the reaction between H_2COO and H_2O.

between the carbon and the terminal oxygen of H_2COO with the OH of water. Our results in Table 1 indicate that the process is exoergic by about 33 kcal mol^{-1} with an activation barrier of 11.3 kcal mol^{-1}. Regarding the transition structure, **TS1** is a five-membered ring and shows how the oxygen of water is linked to the carbon atom (R(CO) = 1.969 Å), while a hydrogen atom is transferred to the terminal oxygen of H_2COO (R(OH) = 1.549 Å). The peroxide OO bond (R = 1.455 Å) has been elongated 0.103 Å with respect to the carbonyl oxide reactant, and the peroxide bond thus loses its double bond character.

In addition to **M2a**, we have also studied several conformational isomers of HMHP (labeled as **M2b–M2e** in Figure 2 and Table 1), which connect HMHP with the final products of its decomposition (see below). These isomers are between 0.2–3.6 kcal mol^{-1} more energetic than **M2a**, and their interconversion barrier is very low [3.3 kcal mol^{-1} for **TS2** (Figure 3), which connects **M2d** and **M2e** (Figure 2 and Table 1)].

C) The unimolecular decomposition of HMHP: We have found four different reaction modes for the unimolecular decomposition of HMHP: (a) and (b) lead to the formation of

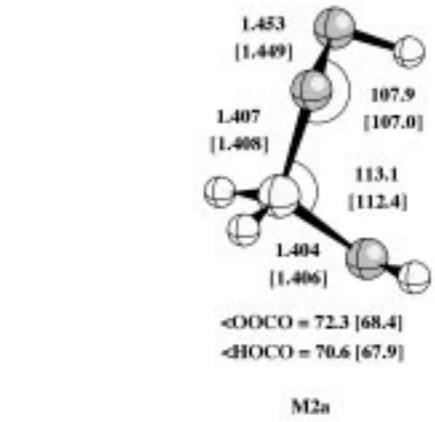

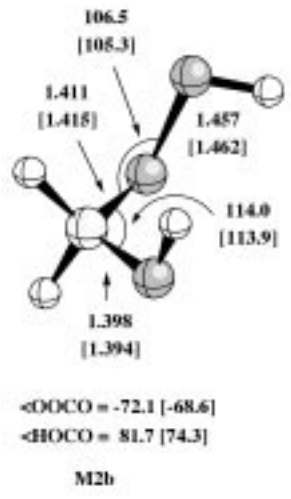

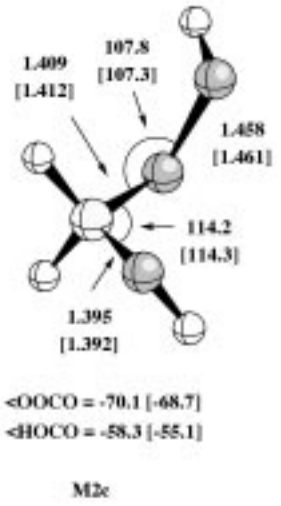

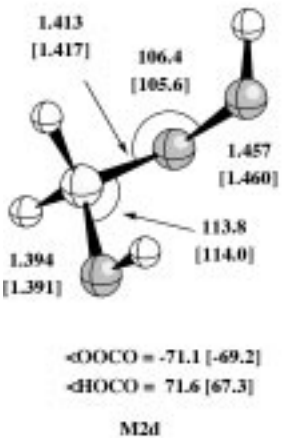

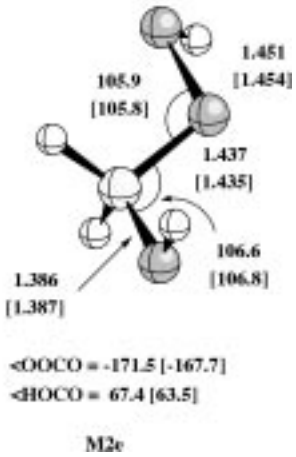

Figure 2. Selected geometrical parameters of the B3LYP/6-311 + G(2d,2p) and B3LYP/6-31G(d,p) (in brackets). **M2a**, **M2b**, **M2c**, **M2d**, and **M2e** for several conformers of HMHP.

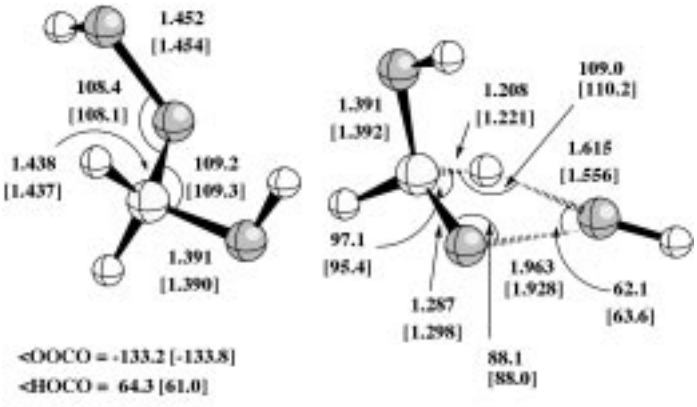

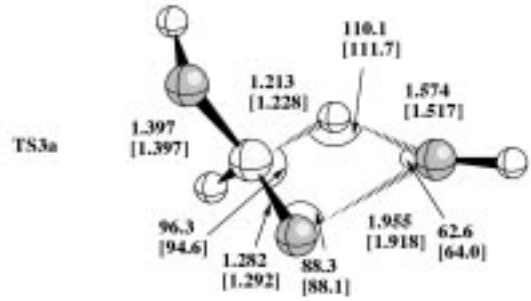

Figure 3. Selected geometrical parameters of the B3LYP/6-311 + G(2d,2p) and B3LYP/6-31G(d,p) (in brackets). **TS2**, **TS3**, and **TS3a** for the stationary points of the reaction between H_2COO and H_2O and the unimolecular decomposition of HMHP.

formic acid (HCOOH) plus H_2O, (c) produces H_2O_2 plus H_2CO, and (d) involves the homolytic cleavage of the hydroperoxide group in HMHP and yields OH and hydroxymethoxy (H_2COOH) radicals.

a) The fate of the first reaction mode is HCOOH plus H_2O and corresponds to the unimolecular decomposition of **M2b**. We have found two different paths (**TS3** and **TS3a**) that produce the s*yn* and *anti* isomers of formic acid, respectively. Both transition structures are four-membered rings and differ only in the orientation of the hydrogen of the hydroxide group. The most relevant geometrical parameters of **TS3** are R(HO) = 1.615 Å, R(HC) = 1.208 Å, R(OO) = 1.963 Å, and R(CO) = 1.287 Å (see Figure 3). The reduction of 0.111 Å in the CO bond with respect to **M2b** shows that the double bond of the formic acid is formed. The large HO bond length (1.615 Å) is similar to that found previously in intramolecular hydrogen transfer from a CH_2 group to an oxygen atom (see for instance **TS6**, **TS12**, and **TS14** from ref. [14] or **TS6** below). Table 1 shows that the computed activation barriers are 44.2 and 47.4 kcal mol^{-1}, respectively; the barrier through **TS3** is slightly smaller than the excess of energy (44.6 kcal mol^{-1}) involved in the HMHP formation (see Table 1 and Figure 6). Thus, we conclude that this path may be active in the gas phase.

b) A second reaction mode for the unimolecular decomposition of HMHP (**M2b**) leads to the formation of *anti*-HCOOH + H_2O, and the corresponding transition structure (**TS4**, Figure 4) involves a five- and a three-membered ring. Figure 4 shows how the OO peroxide bond is broken (R = 1.875 Å) as the hydrogen atom from the hydroxyl group migrates to the terminal oxygen of the hydroperoxide group, and thus one water molecule is formed. At the same time, one hydrogen of the CH_2 moiety migrates to the oxygen, which results from the cleavage of the OO

  0947-6539/01/0710-2230 $ 17.50+.50/0 *Chem. Eur. J.* **2001**, *7*, No. 10

peroxide group (see the three-membered ring part), and this leads to the formic acid molecule. The computed energy barrier is 48.2 kcal mol^{-1}, close to the energy barrier of **TS3a**.

c) The decomposition of HMHP (**M2d**) into $H_2CO + H_2O_2$ is slightly endoergic ($\Delta G_r^{\circ}(298) = 3.3$ kcal mol^{-1}) and has an activation barrier of 47.5 kcal mol^{-1} (**TS5**, Table 1 and Figure 4). This transition structure corresponds also to a four-membered ring, in which the hydrogen of the hydroxide group is transferred to the peroxide oxygen as the CO bond is broken to form the H_2O_2 molecule. The CO bond length of the formaldehyde moiety (1.297 Å, **TS5** Figure 4) is 0.094 Å shorter than the corresponding distance in **M2d**, which shows that the double bond of the aldehyde is formed.

d) Finally, we have also considered the homolytic cleavage of the hydroperoxide group in HMHP that produces OH and hydroxymethoxy (H_2COOH) radicals. Table 1 and Figure 6 show that this is the process that requires the lowest energy in the unimolecular decomposition of HMHP ($\Delta G_r^{\circ}(298) = 27.8$ kcal mol^{-1}), and since **M2** is formed with an excess of energy of about 44 kcal mol^{-1} (see Figure 6), we conclude that *some OH radicals may be released into the atmosphere throughout this mechanism*. Moreover, it is known that the H_2COOH radical reacts with atmospheric O_2 to produce formic acid and OOH radicals.[48, 49] Thus, *the by-reaction between O_2 and H_2COOH will also contribute to the gas-phase formation of formic acid*.

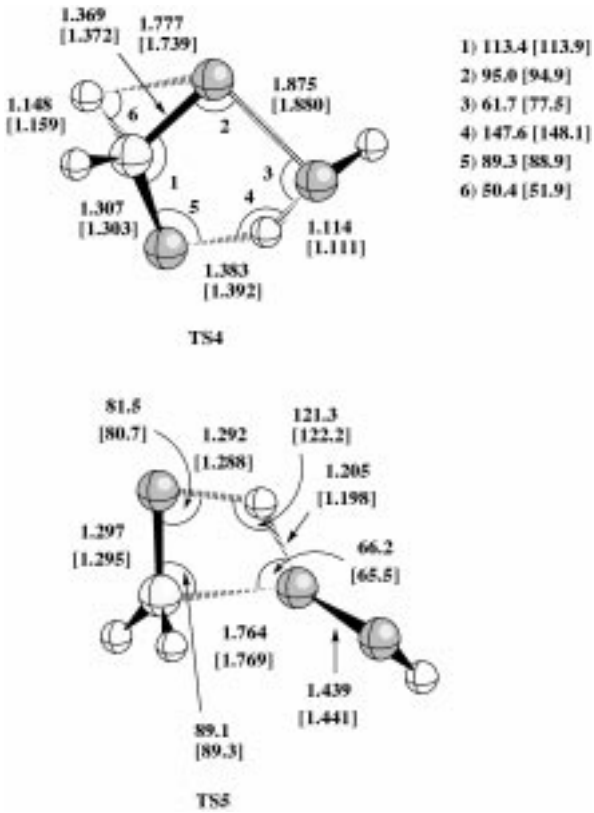

Figure 4. Selected geometrical parameters of the B3LYP/6-311 + G(2d,2p) and B3LYP/6-31G(d,p) (in brackets). **TS4** and **TS5** for the unimolecular decomposition of HMHP.

D) The water-assisted decomposition of HMHP: The experimental results from the literature that refer to the formation and later decay of HMHP[21, 27, 50] indicate that a fraction of the formed compound is collisionally stabilized in the gas phase and can undergo further bimolecular reactions. Therefore, we have also considered *the reaction between HMHP and water*. This process should be highly probable in a water vapor atmosphere, in which the water concentration is very high. For this reaction we have found three different reaction modes [(e), (f), and (g)], which function in the same way as the unimolecular decomposition via **TS3**, **TS4**, and **TS5**, respectively, as described in the previous section. Moreover, with regard to the HMHP moiety, the same bond-breaking/bond-making processes occur as in the unimolecular processes, and the only difference lies in the fact that the hydrogen atoms move through the water molecule. That is, one hydrogen atom from HMHP is transferred to the water molecule while another hydrogen from water is transferred back to HMHP as it decomposes, so that the water molecule is regenerated after the reaction has taken place. In general, the computed activation enthalpies for these HMHP water-assisted decompositions (**TS6–TS8**, Table 1) are between 10 and 25 kcal mol^{-1} smaller than those for the unimolecular processes described above (compare **TS6** with **TS3**, **TS7** with **TS4**, and **TS8** with **TS5**, respectively, for the same processes, non-assisted and water-assisted). Therefore, we could say that this second water molecule produces a catalytic effect in the HMHP decomposition. A similar water catalytic effect on the decomposition of carbonic acid has been recently reported in the literature.[51] However, in the reaction of HMHP with a water molecule there is a significant entropic effect that should be taken into account. Thus, for instance, a ΔS_a of -37 e.u is computed for the reaction between **M2a** + H_2O through **TS6** (this is the difference S(**TS6a**) $- S$(**M2a** + H_2O)) while a ΔS_a of 0.1 e.u is computed for the unimolecular decomposition of **M2b** via **TS3** (this is the difference S(**TS3**) $- S$(**M1b**)); both represent the same process, that is, the production of formic acid plus water. Consequently, the entropic contributions reduce the importance of the water catalytic effect as pointed out for the free-energy values in Table 1.

e) The reaction between HMHP and H_2O via **TS6** and **TS6a** produces HCOOH + 2 H_2O, and has been reported recently by Aplincourt et al.[47] Both transition structures differ in the orientation of the hydroxide group so that **TS6** is the transition state for the **M2a** + $H_2O \rightarrow$ *syn*-HCOOH + 2 H_2O, while **TS6a** is the transition state for the **M2b** + $H_2O \rightarrow$ *anti*-HCOOH + 2 H_2O reaction (see Figure 7). In these processes, one hydrogen of the carbonyl oxide moiety is transferred to the water molecule while one hydrogen from water moves to the terminal oxygen of the peroxide group as the OO bond cleaves (Figure 7). Moreover, with regard to the HMHP moiety, these reactions involve the same bond-breaking/bond-making processes as for **TS3** and **TS3a** in the unimolecular decomposition as discussed in the previous section. Table 1 and Figure 6 show that the computed free-energy barriers for **TS6** and **TS6a** are 44.9 and 47.1 kcal mol^{-1}, respectively; this is of the same order as those of the unimolecular process.

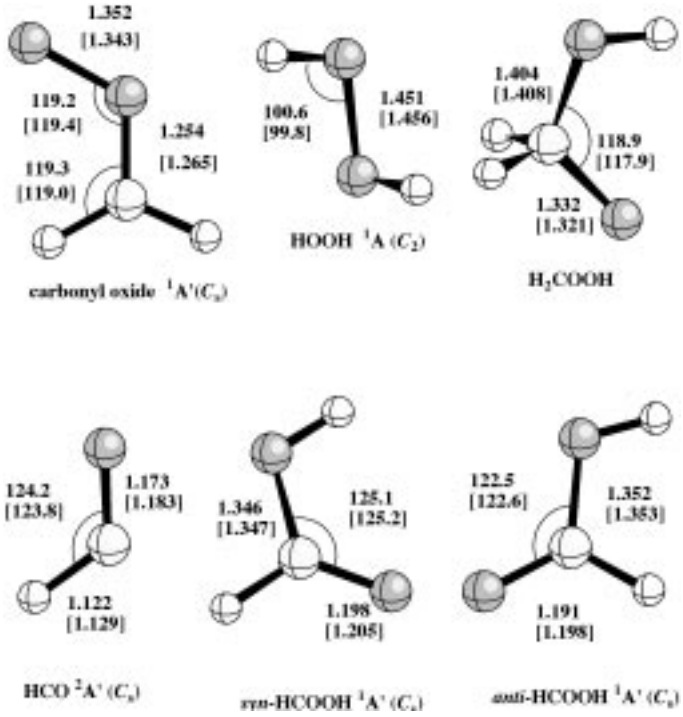

Figure 5. Selected geometrical parameters of the B3LYP/6-311 + G(2d,2p) and B3LYP/6-31G(d,p) (in brackets). Carbonyl oxide $^1A'(C_s)$, HOOH ^1A (C_2), H_2COOH, HCO $^2A'$ (C_s), *syn*-HCOOH $^1A'$ (C_s), and *anti*-HCOOH $^1A'$ (C_s).

f) HMHP, **M2c**, and **M2d** react with H_2O via **TS7** and **TS7a**, respectively, to produce *anti*-HCOOH + 2 H_2O. With regard to the HMHP moiety, these reactions involve the same bond-breaking/bond-making processes that occur in the unimolecular process via **TS4** (see above), and both **TS7** and **TS7a** involve a seven- and a three-membered ring. The activation barriers are computed to be 45.3 and 47.1 kcal mol^{-1} for **TS7** and **TS7a**, respectively, with no significant catalytic effect with respect to the unimolecular process.

g) The last reaction mode between HMHP (**M2e**) and H_2O produces $H_2CO + H_2O_2 + H_2O$. The corresponding transition structure (labeled as **TS8** in Figure 9) is a six-membered ring and constitutes the water catalytic partner of **TS5** in the unimolecular process. The computed free-energy barrier is 33.8 kcal mol^{-1} (Table 1 and Figure 6), which is 13.7 kcal mol^{-1} smaller than that for the unimolecular process via **TS5**. Consequently we observe an important catalytic effect, which makes this *the process with the lowest energy barrier* in the HMHP reaction.

The distinct features of these three reaction mechanisms will enable us to distinguish them easily from one another. If the experiments are performed with D_2O instead H_2O and the origin of the protons that are moved in these processes is taken into account, the reaction through **TS6** and **TS6a** (Figure 7) will lead to HCOOH + HDO. The reaction through **TS7** and **TS7a** (Figure 8) will produce HCOOH + D_2O, and the reaction through **TS8** must produce DOOD + H_2CO + D_2O. Moreover, it is also worth pointing out that the same isotopic effects would occur if the unimolecular decomposition modes through **TS3**, **TS4**, and **TS5**, respectively, were active.

In addition, we have also found a further reaction path, which involves a conformational change in HMHP (from **M2a** to **M2b**) assisted by a water molecule. The corresponding transition structure is labeled as **TS9** in Figure 9 and shows

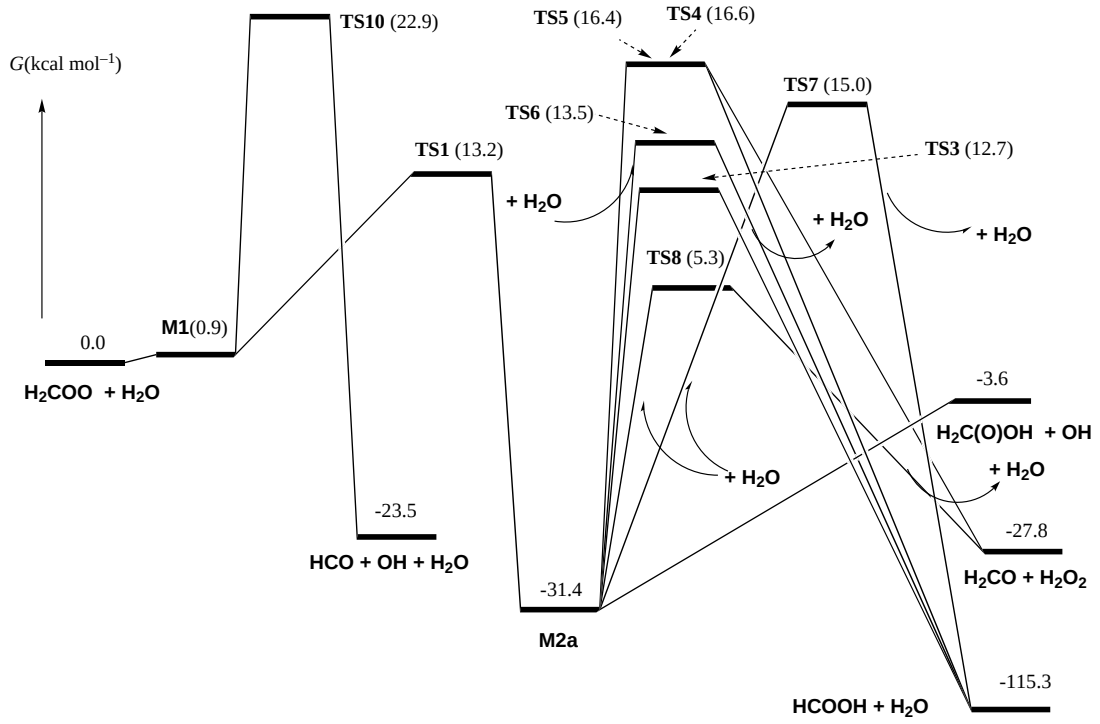

Figure 6. Schematic free-energy diagram for the reaction between H_2COO and H_2O.

0947-6539/01/0710-2232 $ 17.50+.50/0 *Chem. Eur. J.* **2001**, *7*, No. 10

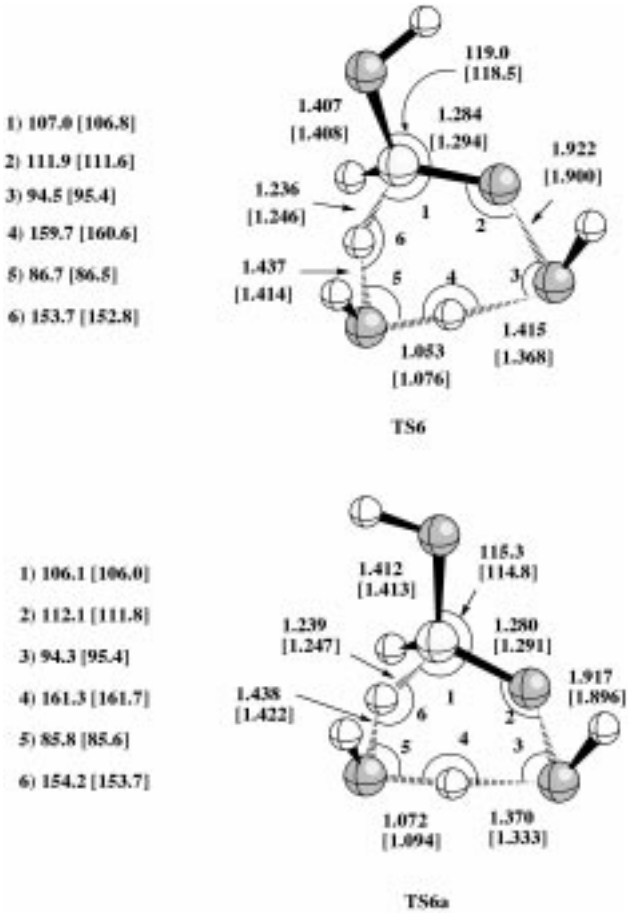

Figure 7. Selected geometrical parameters of the B3LYP/6-311 + G(2d,2p) and B3LYP/6-31G(d,p) (in brackets). **TS6** and **TS6a** for the stationary points of the water-assisted decomposition of HMHP.

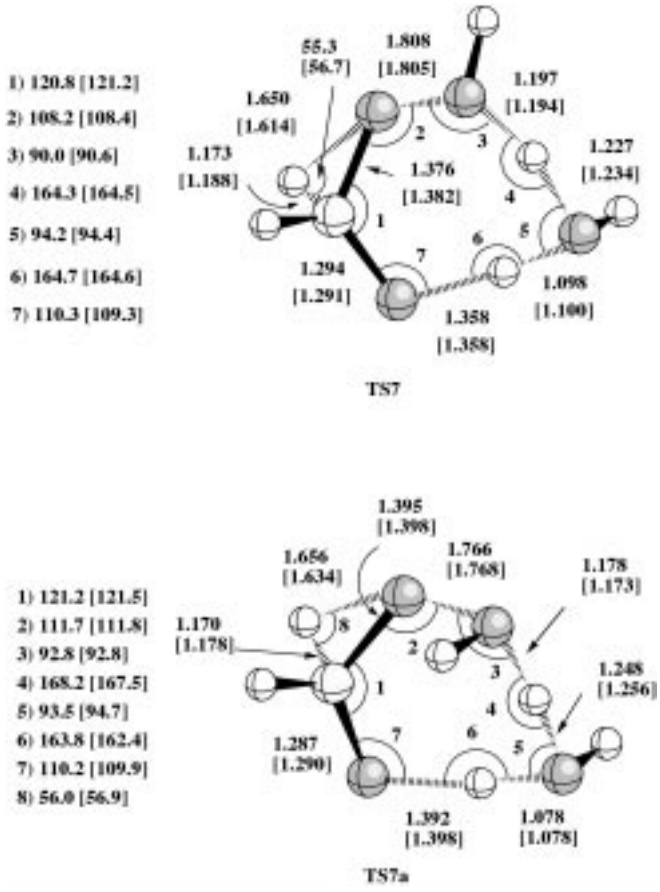

Figure 8. Selected geometrical parameters of the B3LYP/6-311 + G(2d,2p) and B3LYP/6-31G(d,p) (in brackets). **TS7** and **TS7a** for the stationary points of the water-assisted decomposition of HMHP.

how this process implies a migration of three hydrogen atoms. The computed free-energy barrier is 41.5 kcal mol^{-1}, a value that is in the range of the other processes assisted by a water molecule, but it is much more energetic than the paths originated by single bond rotations such as **TS2** (see above), because in this case, bonds have to be broken and formed.

Finally, we comment on a technical point. The geometrical parameters computed at B3LYP/6-31G(d,p) and B3LYP/6-311 + G(2d,2p) agree quite well (see Figures 1–5), and the relative energies obtained at CCSD(T) and B3LYP using the larger basis set differ in the range of 2–5 kcal mol^{-1}. However, the relative energies obtained at B3LYP using the smaller basis set are of lower quality and differ up to 19 kcal mol^{-1} with respect to the CCSD(T) values (see Table 1 and Supporting information); this emphasizes the need to use a large basis set containing diffuse and polarization functions.

E) The water-assisted formation of OH radicals: We have found a further reaction mode between carbonyl oxide and H_2O through the hydrogen-bond complex **M1** that *leads to the formation of HCO + OH radicals.* In this case, the oxygen atom of the water molecule borrows the hydrogen atom of the H_2COO that is placed in the *syn* position, while one hydrogen atom from water is transferred to the terminal oxygen of carbonyl oxide. The corresponding transition state (**TS10**, Figure 10) is a quasiplanar six-membered ring, which shows how the OO bond length (R = 1.453 Å) has been elongated by 0.09 Å from carbonyl oxide. Moreover, the hydrogen atom transferred from water (R(OH) = 1.306 Å) is closer to the terminal oxygen of carbonyl oxide (R(OH) = 1.135 Å), while the hydrogen atom transferred from H_2COO to H_2O is halfway (R(CH) = 1.325 Å and R(OH) = 1.270 Å, respectively). The computed activation free energy (relative to **M1**) is 20.9 kcal mol^{-1}, which is about 10 kcal mol^{-1} higher than the barrier involved in the formation of HMHP via **TS1** (Figure 6 and Table 1). Thus, the high value of this energy barrier makes this process unlikely in the gas phase. A closer look at the geometrical structure of **TS10** in Figure 10 will show us that this process corresponds to a hydrogen-atom migration from the carbon atom to the terminal oxygen in H_2COO, catalyzed by a water molecule. The hydrogen-atom migration in the noncatalyzed path involves a four-membered ring and has been reported by Gutbrod et al.[10] They report an activation barrier of 30.8 kcal mol^{-1} so that the catalytic effect of the water molecule results in a reduction of the barrier of about 9 kcal mol^{-1}. The products of this process are HCO plus OH radicals and one H_2O molecule that is regenerated. In fact our IRC calculations indicate the formation of the carbene HCOOH plus H_2O before the decomposition of HCOOH

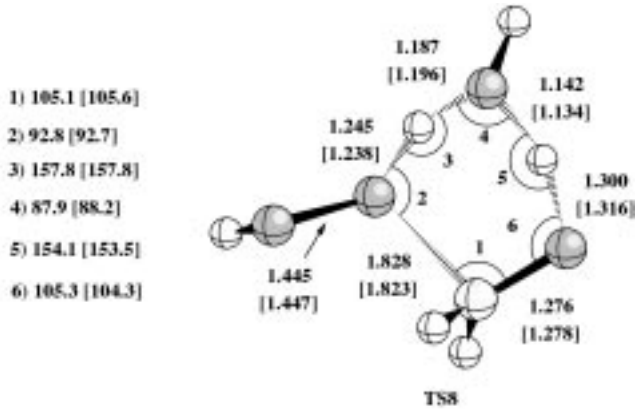

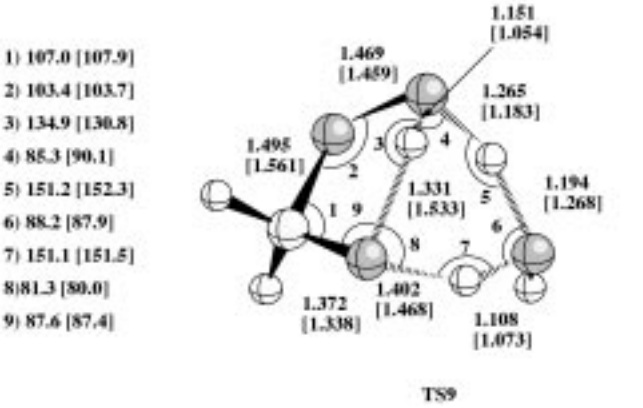

Figure 9. Selected geometrical parameters of the B3LYP/6-311 + G(2d,2p) and B3LYP/6-31G(d,p) (in brackets). **TS8** and **TS9** for the stationary points of the water-assisted decomposition of HMHP.

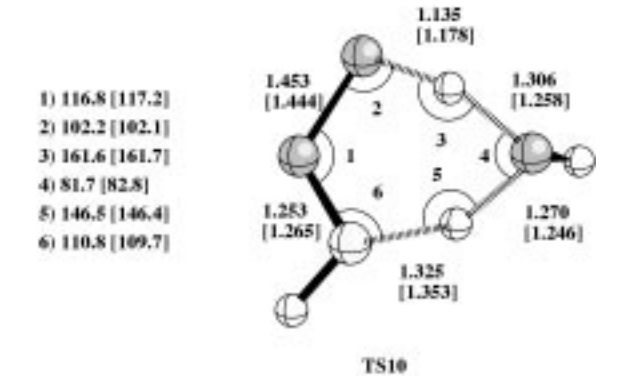

Figure 10. Selected geometrical parameters of the B3LYP/6-311 + G(2d,2p) and B3LYP/6-31G(d,p) (in brackets). **TS10** for the stationary points of the water-assisted decomposition of HMHP.

into HCO + OH. However, Gutbrod et al.[10] showed that this carbene should be unstable so we have considered the final products. Our calculations indicate that the process is exoergic by 25.5 kcal mol^{-1}. As pointed out previously, the features of this reaction mode will allow its easy identification if experiments are carried out with D_2O instead of H_2O. In this case, the isotopic products will be HCO + OD + HDO.

IV. Relevance of these results: There are several points in the results of the present study that are of direct interest for atmospheric chemistry. The first point of interest is the addition of H_2O to H_2COO. The reaction begins with the formation of a hydrogen-bond complex (**M1**) and follows two reaction modes. The energetically most favorable corresponds to the formation of HMHP with a free-energy barrier of 11.3 kcal mol^{-1}. However, it is also of interest for atmospheric chemistry in terms of the second reaction mode, which results in the decomposition of carbonyl oxide into HCO and OH radicals. This reaction path has a high activation barrier (21 kcal mol^{-1}), and therefore it is unlikely that this process occurs in the gas phase. However, this reaction mechanism becomes more important in substituted carbonyl oxides.[49]

The second point of interest refers to the unimolecular decomposition of HMHP. Our calculations indicate that the energetically most favorable path corresponds to the homolytic cleavage of the peroxide OO bond in **M2** that leads to the formation of OH and hydroxymethoxy (H_2COOH) radicals. This decomposition is endoergic by 27.8 kcal mol^{-1}. Since HMHP is formed with an excess of energy of about 44 kcal mol^{-1}, we can conclude that this path will be active in the gas phase. At this point, it is also worth recalling that other mechanisms for the formation of OH radicals in the gas-phase ozonolysis of alkenes have been proposed in the literature.[12, 14, 15, 52] Consequently this process will help to explain the release of OH radicals in the atmosphere as a result of the alkene ozonolysis. Besides the release of OH radicals into the atmosphere by this mechanism, it is also known that the H_2COOH radical reacts with O_2 to form HCOOH.[48] This reaction is very probable in the atmosphere, since O_2 exists in high concentration. Moreover, as a by-product, the highly reactive OOH radical is formed. With regard to other possible decomposition modes of HMHP, our calculations indicate an activation barrier of 44.2 kcal mol^{-1} for the reaction path though **TS3**. Since HMHP is formed with an excess of vibrational energy ($\Delta H_r^\circ(298) = -44.1$ kcal mol^{-1}, see Table 1), we believe that the formation of HCOOH by this mechanism is also energetically feasible. The formation of HCOOH through **TS4** or the formation of H_2O_2 plus H_2CO through **TS5** can be ruled out because these paths require a higher activation energy. These results agree with the experimental observation by Neeb et al.[21] that indicates almost only the formation of formic acid in the decomposition of HMHP.

A third important point derived from the present investigation refers to the reaction between HMHP and a water molecule. Although the enthalpic results displayed in Table 1 indicate a large stabilization in the processes assisted by a water molecule, the consideration of the entropic contribution minimizes this catalytic effect. Thus, only the activation barrier of the path that leads to the formation of H_2CO plus H_2O_2 is significantly reduced and may become active in the gas phase (compare **TS8** with **TS5** in Table 1). In view of this result, one would expect some formation of H_2CO plus H_2O_2. However, Figure 6 shows clearly that the energetic requirements for this process are larger than those for the homolytic cleavage of HMHP that produces H_2COOH + OH, and this makes the formation of H_2CO plus H_2O_2 unlikely. In fact

0947-6539/01/0710-2234 $ 17.50+.50/0 *Chem. Eur. J.* **2001**, *7*, No. 10

Neeb et al.[21] concluded that the formation of these species is of minor importance, and HMHP decomposes to yield almost exclusively formic acid, which agrees with the unimolecular process described above.

Acknowledgements

This research was supported by the Dirección General de Investigación Científica y Técnica (DGICYT, Grants PB98-1240-C02-01 and PB98-1240-C02-02). R.C. thanks the CIRIT (Generalitat de Catalunya, Spain) for financial support. The calculations described in this work were performed on the IBM SP2 and the HP V2500 at the CESCA. We also thank Professor S. Olivella (IIQAB-CSIC) for his valuable suggestions.

[1] F. Su, G. Calvert, H. H. Shaw, *J. Phys. Chem.* **1980**, *84*, 239.
[2] O. Horie, G. K. Moortgat, *Atmos. Environ.* **1991**, *25A*, 1881.
[3] R. Atkinson, *J. Phys. Chem. Ref. Data* **1997**, *26*, 215.
[4] P. Neeb, O. Horie, G. K. Moortgat, *J. Phys. Chem. A* **1998**, *102*, 6778.
[5] O. Horie, G. K. Mortgat, *Acc. Chem. Res.* **1998**, *31*, 387.
[6] J. T. Herron, E. Huie, *J. Am. Chem. Soc.* **1977**, *99*, 5430.
[7] H. Niki, P. D. Maker, C. M. Savage, L. P. Breitenbach, M. D. Hurley, *J. Phys. Chem.* **1987**, *91*, 941.
[8] R. I. Martinez, J. T. Herron, *J. Phys. Chem.* **1988**, *92*, 4644.
[9] D. Cremer, J. Gauss, E. Kraka, J. F. Stanton, R. J. Bertlett, *Chem. Phys. Lett.* **1993**, *209*, 547.
[10] R. Gutbrod, R. N. Schindler, E. Kraka, D. Cremer, *Chem. Phys. Lett.* **1996**, *252*, 221.
[11] J. M. Anglada, J. M. Bofill, S. Olivella, A. Solé, *J. Am. Chem. Soc.* **1996**, *118*, 4636.
[12] R. Gutbrod, E. Kraka, R. N. Schindler, D. Cremer, *J. Am. Chem. Soc.* **1997**, *119*, 7330.
[13] J. M. Anglada, J. M. Bofill, S. Olivella, A. Solé, *J. Phys. Chem. A* **1998**, *19*, 3398.
[14] J. M. Anglada, R. Crehuet, J. M. Bofill, *Chem. Eur. J.* **1999**, *5*, 1809.
[15] S. E. Paulson, M. Y. Chung, A. S. Hasson, *J. Phys. Chem. A* **1999**, *103*, 8127.
[16] K. H. Becker, I. Barnes, L. Ruppert, P. Wiesen in *Free Radicals in Biology and Environment* (Ed.: F. Minisci), Kluwer, Dordretch, **1996**, p. 365.
[17] M. E. Jenkin, S. M. Saunders, M. J. Pilling, *Atmos. Environ.* **1997**, *31*, 81.
[18] R. I. Martinez, J. T. Herron, R. E. Huie, *J. Am. Chem. Soc.* **1981**, *103*, 3807.
[19] S. Gäb, E. Hellpointner, W. V. Turner, F. Korte, *Nature* **1985**, *316*, 535.
[20] K. H. Becker, K. J. Brockmann, J. Bechara, *Nature* **1990**, *346*, 256.
[21] P. Neeb, F. Sauer, O. Horie, G. K. Moortgat, *Atmos. Environ.* **1997**, *31*, 1417.
[22] S. Wolff, A. Boddenberg, J. Thamm, W. V. Turner, S. Gäb, *Atmos. Environ.* **1997**, *31*, 2965.
[23] F. Sauer, C. Schäfer, P. Neeb, O. Horie, G. K. Moortgat, *Atmos. Environ.* **1999**, *33*, 229.
[24] H. Puxbaum, C. Rosenberg, M. Gregori, C. Lanzerstorfer, E. Ober, W. Winiwarter, *Atmos. Environ.* **1988**, *22*, 1841.
[25] E. Hellpointner, S. Gäb, *Nature* **1989**, *107*, 631.
[26] D. Grosjean, *Environ. Sci. Technol.* **1989**, *23*, 1506.
[27] C. N. Hewitt, G. L. Kok, *J. Atmos. Chem.* **1991**, *12*, 181.
[28] E. Sanhueza, M. Santana, M. Hermoso, *Atmos. Environ.* **1992**, *26A*, 1421.
[29] J. E. Lawrence, P. Koutrakis, *Environ. Sci. Technol.* **1994**, *28*, 957.
[30] K. Granby, C. S. Christensen, C. Lohse, *Atmos. Environ.* **1997**, *31*, 1403.
[31] S. Marklund, *Arch. Biochem. Biophys.* **1973**, *154*, 614.
[32] D. Möller, *Atmos. Environ.* **1989**, *23*, 1625.
[33] C. N. Hewitt, G. L. Kok, R. Fall, *Nature* **1990**, *344*, 56.
[34] P. Dowideit, C. von Sonntag, *Environ. Sci. Technol.* **1998**, *32*, 1112.
[35] S. Hatakeyama, H. Bandow, M. Okuda, H. Akimoto, *J. Phys. Chem.* **1981**, *85*, 2249.
[36] P. Neeb, O. Horie, G. K. Moortgat, *Tetrahedron Lett.* **1996**, *37*, 9297.
[37] R. Atkinson, *Atmos. Environ.* **2000**, *34*, 2063.
[38] A. D. Becke, *J. Chem. Phys.* **1993**, *98*, 5648.
[39] P. C. Hariharan, J. A. Pople, *Theor. Chim. Acta* **1973**, *28*, 213.
[40] A. P. Scott, L. Radom, *J. Phys. Chem.* **1996**, *100*, 16502.
[41] R. Krishnan, J. S. Binkley, R. Seeger, J. A. Pople, *J. Chem. Phys.* **1980**, *72*, 650.
[42] J. Cizek, *Adv. Chem. Phys.* **1969**, *14*, 35.
[43] R. J. Barlett, *J. Phys. Chem.* **1989**, *93*, 1963.
[44] K. Raghavachari, G. W. Trucks, J. A. Pople, M. Head-Gordon, *Chem. Phys. Lett.* **1989**, *157*, 479.
[45] S. F. Boys, F. Bernardi, *Mol. Phys.* **1970**, *19*, 553.
[46] M. J. Frisch, G. W. Trucks, H. B. Schlegel, P. M. W. Gill, B. G. Johnson, M. A. Robb, J. R. Cheeseman, T. Keith, G. A. Petersson, J. A. Montgomery, K. Raghavachari, M. A. Al-Laham, V. G. Zakrzewski, J. V. Ortiz, J. B. Foresman, J. Cioslowski, B. B. Stefanov, A. Nanayakkara, M. Challacombe, C. Y. Peng, P. Y. Ayala, W. Chen, M. W. Wong, J. L. Andres, E. S. Replogle, R. Gomperts, R. L. Martin, D. J. Fox, J. S. Binkley, D. J. Defrees, J. Baker, J. P. Stewart, M. Head-Gordon, C. Gonzalez, J. A. Pople, *Gaussian 94*, Gaussian, Inc., Pittsburgh, PA, (USA), **1995**.
[47] P. Aplincourt, M. F. Ruiz-López, *J. Am. Chem. Soc.* **2000**, *122*, 8990.
[48] J. P. Burrows, G. K. Moortgat, G. S. Tyndall, R. A. Cox, M. E. Jenkin, G. D. Hayman, B. Veyret, *J. Phys. Chem.* **1989**, *93*, 2375.
[49] Unpublished results from our laboratory.
[50] F. Su, J. G. Calvert, J. H. Shaw, *J. Phys. Chem.* **1979**, *83*, 3185.
[51] T. Loerting, C. Tautermann, R. T. Kroemer, I. Kohl, A. Hallbrucker, E. Mayer, K. R. Liedl, *Angew. Chem.* **2000**, *112*, 920; *Angew. Chem. Int. Ed.* **2000**, *39*, 892.
[52] M. Olzmann, E. Kraka, D. Cremer, R. Gutbrod, S. Andersson, *J. Phys. Chem.* **1997**, *101*, 9421.

Received: October 4, 2000 [F2774]